Urban Climate News

Quarterly Newsletter of the IAUC

ISSUE NO. 60 JUNE 2016 • www.urban-climate.org • INTERNATIONAL ASSOCIATION FOR URBAN CLIMATE

From the IAUC President

Colleagues – welcome to the 60th issue of the *Urban Climate News*. This issue includes a feature article by IAUC Secretary David Sailor and colleagues on "An Anthropogenic Heating Database for US Cities", an urban project report by ICUC-9 student award winner Patricia Drach with co-author Rohinton Emmanuel, and a special report on the installation of an urban weather station on the Mount of Olives in Jerusalem. Thanks to all the issue contributors and to our editor, David Pearlmutter.

Once again, I raise the theme of cities and climate change, because of events in Canada that occurred since the last edition of the *Urban Climate News*. In early May, a growing wildfire in Alberta, Canada forced the entire evacuation of the town of Fort McMurray. More than 80,000 people were forced to leave on short notice. The fire entered the town and resulted in the loss of 2,400 structures, about 10 per cent of the city's buildings, with many others damaged. Several neighbourhoods suffered nearly total loss and it is not clear if those areas will be rebuilt. Firefighting efforts and maintenance of the town's water system avoided an even greater loss, and no human fatalities were incurred from the fire. The early season wildfire was aided by abnormally warm and dry conditions for the time of year.

This event has brought a heightened awareness in Canada to the environmental hazards faced by cities and how they may change with large scale climate warming. It also illustrates the broad range of environmental considerations that urban climate planning and design must take into account. In addition to the planning and design considerations directed towards local scale climates that seek to reduce extreme conditions and provide benefits such as improved air quality and energy efficiency, we must also consider the landscape and climate surrounding the city and how these may change under future climate scenarios.

It is not clear to what extent urban climate design principles may be considered as Fort McMurray enters its recovery phase. A limiting factor is that infrastructure, such as roads, sewers, gas and water supply, remain in place and may limit the scope of possible interventions. Another is the toxicity of the land following the fire that may limit habitation in some areas. And the city is located in a climate zone that experiences hot summers and cold winters that themselves provide some conflicting needs when considering urban climate design. So planning and design considerations that might be typical for this high latitude (56.7°N) city, such as closely spaced buildings to reduce winter time heat loss and use of vegetation as windbreaks, must also consider the potential contradictions associated with increased risk of rare but extreme events such as wildfires. For cities in forested high latitude biomes that may be subject to greater risk of summer wildfires, the impact of degraded air quality that is associated with fires that remain a substantial distance away is also a concern. A combined heatwave and wildfire event that affected Moscow and other Russian cities in the summer of 2010 resulted in significant excess mortality, another example of such extra-urban events that have had significant impact on cities and their residents. Such events serve as a reminder that in considering urban climate design and planning we must be cognizant of our larger scale surroundings, their potential influence on urban climates, and importantly, a consideration of future climate scenarios that affect both.

– James Voogt,
IAUC President

javoogt@uwo.ca

Inside the Summer issue...

2 **News:** Mapping urbanization • Birds stressed out • India forests 200 cities

6 **Feature:** A new anthropogenic heating database developed for US cities

11 **Projects:** The microclimatic effects of urban form and atmospheric stability

18 **Special Reports:** Climatic "memory": The ancient olive trees of Jerusalem

20 **Bibliography:** Recent publications
Conferences: Upcoming gatherings

23 **IAUC Board:** IAUC has signed a new agreement of cooperation with WMO

The rise and fall of great world cities: 5,700 years of urbanisation – mapped

Recent research provides a better understanding of urban populations throughout history, digitising almost 6,000 years of data for the first time

June 2016 — Urbanisation is one of the defining processes of modern times, with more than half of the world's population now living in cities, and new mega-metropolises mushrooming in Asia, Latin America and Africa. But a comprehensive, digitised database of city populations through world history has been lacking, with the United Nations' dataset only extending as far back as 1950.

That was until recent research, published in the journal *Scientific Data*, transcribed and geocoded nearly 6,000 years of data (from 3700BC to AD2000). The report produced a gargantuan resource for scholars hoping to better understand how and why cities rise and fall – and allowed blogger Max Galka to produce a striking visualisation on his site Metrocosm.

"In general, it helps us see human interaction with the environment," says lead author Meredith Reba of the Yale School of Forestry and Environmental Sciences. "It helps us to understand why settlements grew at the times they did."

Mining tabular data from two tomes only available in print (the works of historian Tertius Chandler and political scientist George Modelski), Reba and her team mapped how city populations developed around the world over the millennia (see maps on page 3). The resulting dataset – available for free online – bills itself as "a first step towards understanding the geographic distribution of urban populations throughout history and around the world."

The Sumerian city of Eridu marks the dawn of urbanisation in 3700BC, which trickles around Mesopotamia, Iran, India and China before eventually coming west to the Mediterranean. Mapping the data makes certain trends and patterns quite clear. For instance, it's notable that the earliest cities from China to Mesoamerica can all be found in a similar latitudinal belt, suggesting a possible link between early phases of urbanisation and climate.

Many more urban centres sprang up around the world thereafter but, as late as 1800, only 3% of the world's population lived in cities. Global urbanisation accelerated from the middle of the 19th century onwards. This precipitous rise is palpable in Galka's visualisation of the data (and in this one by Quartz), with a burst of cities clotting the map around 1875 and then again during the 20th century.

The last entries in the database date to 2000AD; if updated to the present day, the database would include the stratospheric 21st-century growth in urban populations in Asia. Reba admits that the data "is not final in any sense. Our aim was to pull together a richer, global urban population database, and to get this data into a usable format so it can be tested and improved."

Watch as the world's cities appear over 6,000 years. *Source:* www. theguardian.com

Though the report offers no theories of its own, Reba and her team hope that the results of their work will help researchers better explore a range of subjects that have long troubled scholars of urbanisation. Reba's initial motivation for the study was her frustration at the lack of data relating to her own field of interest – the relationship between the growth of cities and their proximity to agricultural land. But combined with other data and lines of inquiry, the database can be used to trace deeper ecological and climatic trends, as well as to study the effect of transport, trade routes, and shifting political boundaries on urban growth.

Reba didn't try to reconcile the multiple definitions of a city in Chandler and Modelski's works, which vary significantly by region and period. Chandler, for instance, generally considered any locality of greater than 20,000 people between AD800-1850 to be worthy of recording, but only counted places in Asia with a population of over 40,000 in that same period. Modelski's minimum thresholds changed over time: at least 10,000 inhabitants until 1000BC, 100,000 until AD1000, and one million people thereafter. They amassed their figures for urban populations from a plethora of sources, including censuses, traveller's accounts, tax rolls, gazetteers, disaster records, public bath rolls and archaeological records.

Though there is thorough data for a handful of Chinese localities, the new database is much more comprehensive in how it charts European urban development than the waxing and waning of cities in South Asia, Africa, and pre-Columbian America. "There's definitely a Eurocentric view," Reba says, but she hopes new archeological and archival discoveries will help expand the database, and begin to fill in the more glaring geographic and temporal gaps. —*Source:* https://www.theguardian.com/cities/2016/jun/27/rise-fall-great-world-cities-5700-years-urbanisation-mapped

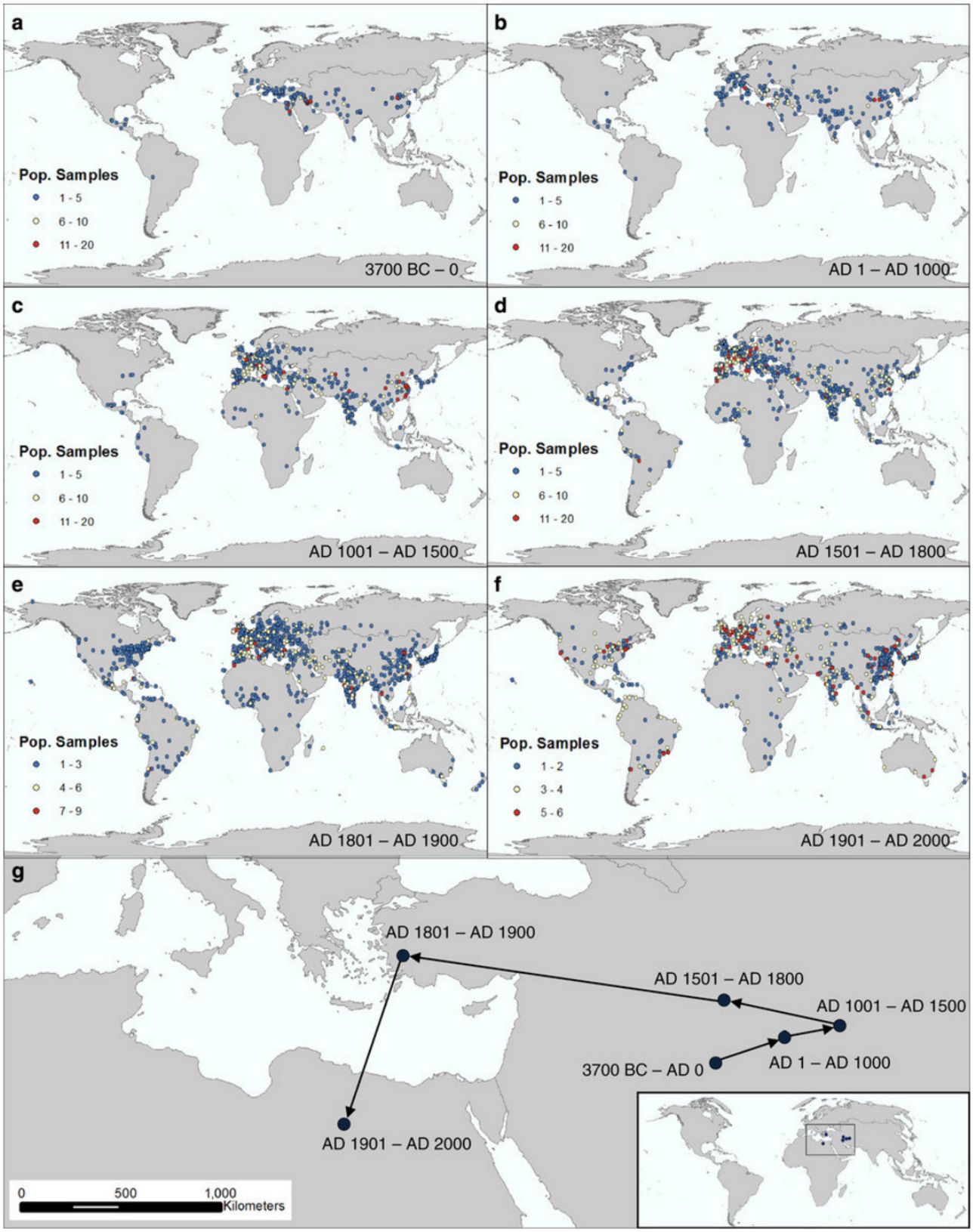

Spatial and Temporal Representation – Global View of Data Points. (a–f) illustrate both the spatial and temporal frequency of city-level population points for different time periods. (a–d) represent the pre-modern period, from 3700 BC–AD 1800, and use the same scale to measure frequency of data points per city. (e,f) represent the modern period and shorter time frame per period and therefore the frequency scale is shorter and separated into thirds. (g) illustrates global mean centers (GMCs) for the same time periods. Each GMC is weighted by city population for each data point and was calculated and is pictured in the Goode Homolosine projection. *Source:* http://www.nature.com/articles/sdata201634

The urban environment is stressing some birds to death

Simply growing up in cities can have a detrimental effect, say researchers

Urban Great Tit reared in rural environment (left) and rural Great Tit reared in urban environment (right). Photos by P. Salmon. *Source:* www.citylab.com

June 2016 — Urban spaces can be a boon to wildlife. Thanks to the heat-island effect, they're often warmer than the woods. And human garbage makes for easy eatin', as anybody who's seen a pigeon plumped into a feathery balloon from stale hot-dog buns knows.

But there's also evidence cities harm animals—artificial lights can addle entire ecosystems, for example, and glass architecture kills millions of migrating birds each year. Now researchers in Sweden are spreading the dismal word that by simply being born in cities, certain kinds of birds are doomed to a heightened risk of premature death.

Pablo Salmón at Lund University and others wanted to see if *Parus major*, aka the great tit, fared any differently whether it grew up in a city or rural environment. So they took bird siblings and had one group reared in the countryside and the other in Malmö, then tested their blood about two weeks later for changes to the animals' telomeres.

A telomere is a string of DNA dangling from the end of a chromosome that's a "suggested biomarker of longevity," write the researchers. Blood sampling revealed the urban bird–s had shorter telomeres compared to their rural kin. Here's more from a university press release:

> *According to the researchers, the induced stress that the urban great tits are experiencing is what results in shorter telomeres and thereby increases their risk of dying young….*
>
> *"Although there are advantages to living in cities, such as the access to food, they seem to be outweighed by the disadvantages, such as stress—at least in terms of how quickly the cells of the great tits age," says biologist Pablo Salmón who conducts research in the field of evolutionary ecology at the Faculty of Science, Lund University.*

The scientists say they were "surprised" to find this ostensibly irreversible change had occurred in such a short time. The next step might be to test other creatures for telomere abnormalities, Salmón adds, as these "results also raise questions concerning the aging of other animals affected by urbanization, and humans for that matter." *Source:* http://www.citylab.com/weather/2016/06/birds-city-health-research-lund-university/487967/

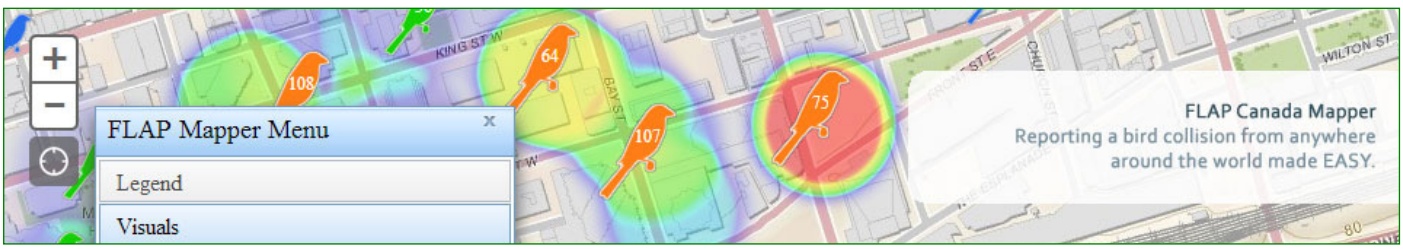

The FLAP Mapper is a web application designed to help users around the world report bird collisions with buildings. See: http://flap.org/mapper_guide.php

Environment Ministry of India to create urban forests in 200 cities to increase green cover and protect wildlife

June 2016 — On World Environment Day, the Indian Minister for Environment, Forests and Climate Change, Mr. Prakash Javadekar, highlighted the need for increasing the green cover and protecting wildlife.

"Urban forestry is the new thrust area and we will be taking up a massive tree plantation drive in as many as 200 cities and towns across the country," said Mr. Javadekar at a commemorative function organized at the Sanjay Gandhi National Park in Borivali, Mumbai. The Environment Ministry will launch the Urban Forestry Scheme in Pune, where 6000 saplings will be planted to create an urban jungle on about 80 acres of land.

Mr. Javadekar observed that in most cities there are gardens and parks but no forests. There are many cities where the forest department has its land but there are no forests on it or they are degraded. "In these places, through peoples participation, we will establish urban forestry," he added. Stressing that the green mission can succeed only through people's active participation, the Environment Minister urged the citizens to plant trees, take a selfie and share photographs on the ministry's web site.

Drawing attention to this year's theme of the World Environment Day, "Go Wild For Life," Mr. Javadekar underlined the government's resolve for protection of wildlife. He said the Government began this year's World Environment Day celebrations by launching Asia's first Vulture Re-introduction Programme at Pinjore in Haryana. Mr. Javadekar said vultures, the true Swachch Bharat volunteers, had become endangered since 1990, after eating carcasses of cattle which were injected with Diclofenac, a pain killer drug. "We had more than 4 crore vultures in the country, now not even 4 lakh are left," he said.

Speaking about wildlife protection, Mr. Javadekar asserted that trade in wildlife products should be completely stopped. He said the Government has also initiated proactive measures for protection of wildlife and informed that shoot on sight orders given to armed guards at the Kaziranga National Park in Assam had resulted in the death of 24 poachers. He appealed to the people not to buy any product made from wild animal body parts. "If there is no market for the products, poaching will end automatically," he remarked. The Minister later symbolically burnt the confiscated wildlife products in the open, to send a message to end the wildlife trafficking.

Mr. Javadekar said that with better understanding and awareness, man and wildlife can live in harmony. He said most tribals, who live on the edges of forests, live in harmony with nature.

One year ago, the environment minister said the envisioned forestry scheme will act against climate change by creating a carbon sink and against air pollution in cities. He added that the ministry was also considering starting tree surveys in cities which can be conducted by residents and college or school students. A plan was being worked on to create small nurseries of about 1000 to 2000 plants in government schools where there is some extra space. *Source:* http://www.business-standard.com/article/government-press-release/environment-ministry-to-create-urban-forests-in-200-cities-to-increase-116060500745_1.html

"The best time to plant a tree was 20 years ago. And the next best time is today." **This Chinese proverb has inspiried action, with the planting of 4000 trees at SmritiVan (A Forest of Memories) in the heart of city of Pune, India. "Urban forests are the essential lungs of the cities and provide a wide range of ecosystem services like clean air and water, tempered floods, food, and biodiversity", stated Rajendra Shende, Chairman of TERRE. "The breadth of ecosystem services provided by nature is often undervalued if we consider reduction in noise, increased physical and psychological wellbeing, regulation of the local climate, sequestration of CO_2 and provision of renewable energy", he added.**

An Anthropogenic Heating Database for US Cities



By David J. Sailor[1] (dsailor@asu.edu), **Matei Georgescu**[1] **and Melissa A. Hart**[2]

[1] Arizona State University, Tempe AZ, USA

[2] University of New South Wales, Sydney, Australia

Introduction

There is growing interest and need for quantification of anthropogenic waste heat emissions for use in modeling of urban climates. These emissions arise from vehicles, energy use in buildings/industry, and human metabolism. As anthropogenic heat flux (Q_f) is directly tied to the spatial density of energy consumption, it varies depending upon the scale of analysis. Thus, at country and continental scales anthropogenic heat emissions are typically less than 1 W/m^2 (Flanner, 2009). Greater population density at city scales results in Q_f values in the range of 10-100 W/m^2 (Klysik, 1996; Sailor and Lu, 2004). When averaged over even finer scales, such as the central business districts of dense cities such as Tokyo, it is not uncommon for anthropogenic heating magnitudes to locally exceed 1000 W/m^2 (e.g. Ichinose et al., 1999). The anthropogenic heating database resource discussed in this article is intended for application at the city-scale, although methods are available for disaggregating it for use at finer scales.

Anthropogenic heating can be a significant component of the urban energy budget, so it is important to include this heat source in models of the urban climate. Regional atmospheric modeling systems such as the Weather Research and Forecasting model (WRF) provide default anthropogenic heating profiles (independent of season) scaled by a magnitude parameter (in WRF, these default values are 90, 50, and 20 W/m^2 respectively for commercial, high-density residential, and low-density residential urban land categories). While these profiles are user-editable, the lack of available anthropogenic heating data for many cities increases the likelihood that users simply use the profiles unchanged. Alternatively, some atmospheric models such as WRF include the option of incorporating simplified building energy consumption models that account for waste heat from buildings. However, such methods ignore emissions from transportation and industry.

To address the need for city-scale data for total anthropogenic waste heat emissions we have applied the methodology of Sailor and Lu (2004) to develop month-specific Q_f profiles for 61 of the largest US cities. We have further generalized the results from this effort so that it can readily be applied to any city internationally. The methods for this national anthropogenic heating database are fully described in our recent (open-access) publication in *Atmospheric Environment* (Sailor *et al*., 2015). All results from the application of this method to the 61 US cities are available online at geoplan.asu.edu/research-and-outreach/projects/AHdata. For the purposes of this article, data from a subset of these cities are presented.

Summary of Methodology

The method used in this study is based on the work published in Sailor and Lu (2004) and is described in detail in Sailor *et al*. (2015). A brief summary of methods is presented here for reference. As a starting point, Q_f is divided into three components representing the major sources of waste heat in the urban environment: vehicles, building/industry energy use, and human metabolism. The building/industry sector can be further divided into heat rejected directly from electricity consumption and heat released from point-of-use heating fuels such as natural gas and fuel oil.

Each component of the anthropogenic heating profile is based on a population density formulation. We first calculate per capita energy intensity for the city and sector and then multiply this value by the population density. This method also corrects for variations in weather from the state-level to the city-scale. Specifically, we developed re-

gression models relating state-level degree-days to state-level consumption data, and applied these to the corresponding city-level degree-day data (Sailor and Vasireddy, 2006). The method can be further refined by applying diurnally-varying population density, as there is often a significant flux of population into urban centers during work hours.

Data Resources

We used population-weighted state values of monthly cooling and heating degree-days, from NCDC (series 5-1, 5-2; 2010). For the city-level degree-day data we used the station normals database (Arguez *et al*., 2012). From these sources we extracted the year 2010 specific monthly heating and cooling degree-days for all cities and states involved in our analysis.

For human metabolism we assumed a representative diet of 2400 kCal and nocturnal and daytime metabolic rates of 70 and 140 watts, respectively. Metabolic rates were then multiplied by population density to arrive at an estimate of anthropogenic heating from human metabolism.

State-level aggregated monthly totals of electricity consumption (and other fuels) were obtained from the US Department of Energy's Energy Information Administration (EIA 2010a, EIA 2010b). State-level data were scaled to reflect weather-related differences at the city scale, and then mapped onto diurnal profiles (Sailor and Lu, 2004).

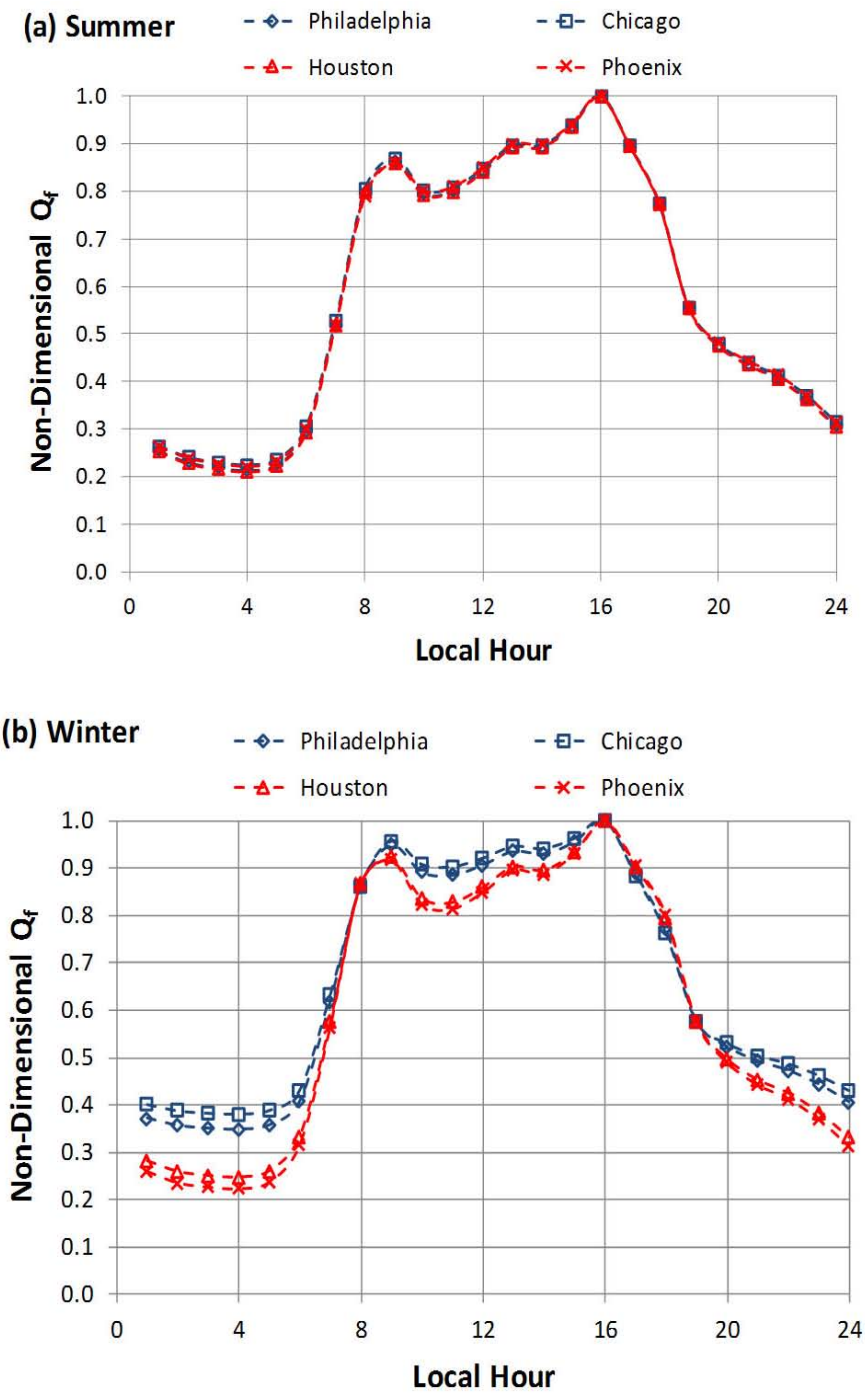

Figure 1. Representative non-dimensional (a) summer (July) and winter (January) anthropogenic heating profiles for the two warm winter climate cities of Phoenix and Houston and for the two cold climate cities of Philadelphia and Chicago.

To estimate heat released from vehicles we used US Department of Transportation annual summaries of Daily Vehicle Miles Traveled (DVMT) for major urbanized areas (US DOT, 2013). The hourly profile for vehicle emissions was estimated using the national profile created by Hallenbeck *et al*. (1997), using energy release per vehicle per km of travel of 3605 kJ/km.

Results

The anthropogenic heating database project for US cities is implemented through a set of twelve monthly spreadsheets that provide hourly anthropogenic heating estimates for each of the 61 cities. These data have been compiled both at the city and greater metropolitan scales. The vast majority of the cities analyzed had anthropogenic heating profiles that peak in winter. In fact, only ten cities in the states of Florida, California, Arizona, Nevada, Texas, and Louisiana had summer-peaking profiles. However, it was found that summertime anthropogenic heating profiles have a common shape regardless of the underlying climate. Wintertime profiles, on the other hand, show more dependence on climatic region. Two clusters of profiles resulted, one for cities with cold winter climates (annual heating degree days > 4000°C-day, using an 18.3°C base) and one for cities with warm winter climates. This suggests that it is reasonable to define two non-dimensional profiles for anthropogenic heating in winter – one that applies to warmer cities, and one for colder cities.

Table 1. Hourly non-dimensional profile function values for the universal summer (August) profile and the two winter (January) profiles. Cold winter cities have annual HDD > 4000°C-day (18.3°C base).

Hour	Summer Profile	Winter Profile	
		Cold winter cities	*Warm winter cities*
1	0.25	0.37	0.28
2	0.23	0.35	0.26
3	0.25	0.35	0.25
4	0.21	0.34	0.25
5	0.22	0.35	0.26
6	0.29	0.40	0.34
7	0.53	0.62	0.58
8	0.82	0.86	0.87
9	0.87	0.95	0.92
10	0.80	0.89	0.84
11	0.80	0.88	0.83
12	0.84	0.91	0.86
13	0.89	0.93	0.90
14	0.89	0.93	0.90
15	0.93	0.96	0.93
16	1.00	1.00	1.00
17	0.90	0.89	0.90
18	0.78	0.77	0.79
19	0.56	0.58	0.57
20	0.48	0.52	0.50
21	0.44	0.49	0.45
22	0.41	0.47	0.43
23	0.36	0.44	0.39
24	0.30	0.40	0.33

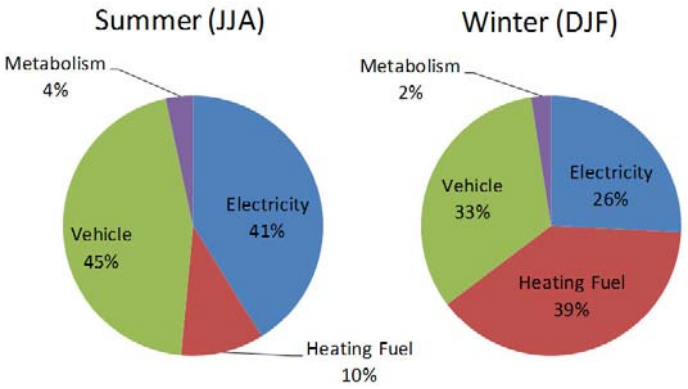

Figure 2. Relative contributions of sectors in 61 largest US cities to total anthropogenic heating in summer and winter.

Non-dimensional anthropogenic heating profiles (hourly values divided by daily maximum) are illustrated in Fig. 1 for four representative cites. Two of these cities are cold winter climate cities – Philadelphia and Chicago; while the other two are warm cities – Houston and Phoenix. Clearly, the non-dimensional summer profiles are similar, peaking at 4 pm local time. In winter, all profiles still peak at 4 pm local time. However, the cold winter climate cities have slightly less variability in energy consumption throughout the day in winter. The average numeric values of these non-dimensional profiles based on data from all 61 cities are summarized in Table 1.

These hourly profile values can be multiplied by the corresponding $Q_{f,max}$ value for the city and season of interest to arrive at anthropogenic heating profiles representative of specific cities in the US. Table 2 presents $Q_{f,max}$ values for a sample of 25 cities selected from the larger data base.

Fig. 2 presents a comparison of the relative contribution that each component (vehicles, electricity, heating fuels, and metabolism) makes to the total anthropogenic heating profile across all cities. As would be expected, the heating fuel contribution is largest in winter and smallest in summer, and the contribution from electricity use is largest in summer and smallest in winter. The relative contributions from the vehicle sector and metabolism increase in summer since the total anthropogenic heating is largest in winter. However, waste heat

Table 2. Maximum values of Q_f for the daily profiles of city-scale anthropogenic heating in summer (August) and winter (January) for a sample of 25 of the cities in the data base.

City	State	$Q_{f,max}$		Winter profile
		Summer (W/m²)	*Winter (W/m²)*	
Atlanta	GA	11.9	13.3	Warm
Baltimore	MD	25.5	34.9	Cold
Boston	MA	41.1	62.3	Cold
Chicago	IL	34.6	57.5	Cold
Dallas	TX	14.0	14.3	Warm
Denver	CO	11.8	15.7	Cold
Detroit	MI	16.9	26.2	Cold
Houston	TX	13.0	12.6	Warm
Las Vegas	NV	15.4	14.2	Warm
Los Angeles	CA	21.5	22.6	Warm
Miami	FL	34.5	29.8	Warm
Minneapolis	MN	23.9	36.5	Cold
Nashville	TN	5.7	6.4	Warm
New Orleans	LA	7.3	7.1	Cold
New York	NY	62.9	96.6	Cold
Philadelphia	PA	34.2	49.0	Cold
Phoenix	AZ	9.2	7.7	Warm
Sacramento	CA	12.4	13.9	Warm
Salt Lake City	UT	4.9	6.6	Cold
San Diego	CA	10.8	11.2	Warm
San Francisco	CA	42.8	48.5	Warm
Seattle	WA	23.1	28.2	Warm
St. Louis	MO	20.8	26.0	Warm
Toledo	OH	11.8	17.9	Cold
Washington	DC	41.9	54.4	Cold

emission from metabolism is an order of magnitude smaller than that of the other sources. This figure underscores the importance of including emissions from buildings/industry as well as transportation.

Estimation Process for Other Cities

A stepwise multiple regression analysis was applied to all monthly data from the 61 cities to quantify the relative importance of the factors that influence anthropogenic heat. This facilitates development of a predictive model of maximum Q_f for each season that can be applied to other cities, for which the required data for the more detailed approach are not available. From the independent variables included in our analyses (HDD, CDD, DVD, population density), a final set of models was determined for each season. The final predictive models are:

$$Q_{f,max\ (winter,\ spring,\ autumn)} = \beta 0 + PopDens * \beta 2 + HDD * \beta 1 \quad (1)$$

$$Q_{f,max\ (summer)} = \beta 0 + PopDens * \beta 2 \quad (2)$$

where degree day variables are monthly totals in °C-days, based on a threshold temperature of 18.3°C and *PopDens* is the population density in persons per square kilometer. Note that there was a typographical error in the corresponding equations presented in Sailor *et al*. (2015). The seasonal values for the regression coefficients are given in Table 3 along with Root Mean Square Error (RMSE) and R^2 values. The predicted value of maximum Q_f can be applied to the appropriate universal profile to estimate diurnal profiles for each season of the year.

The value of $Q_{f,max}$ arrived at through application of Eqs. 1 and 2 may significantly overestimate anthropogenic heating in cities within other countries where differences in infrastructure, end-use efficiency, and demographics result in lower per capita consumption rates. Therefore, a correction factor applied to the results provided by Eqs. 1 and 2 is necessary, to account for the fact that individuals in

a non-US city would consume energy at a different rate than their counterparts in similar US climates.

As a first order correction we can compare the ratio of per capita energy consumption in the target country to that in the US. The most readily available data for this purpose are energy consumption totals that can be converted to equivalent barrels of oil use per person and then non-dimensionalized by dividing by the US consumption rate. Sample international city multipliers (f_{ec}) are provided in Sailor *et al*. (2015, Table 5). This ratio can be applied as a straightforward multiplier to the value of $Q_{f,max}$ obtained from Eqs. 1 and 2. See the full *Atmosperic Environment* article (Sailor *et al*., 2015) for a complete description of the extrapolation method and results for non-US cities.

Table 3. Coefficients for regression models (Eqs. 1 and 2) for seasonal maximum anthropogenic heating results for all 61 cities.

Month	β_0	β_1	β_2	RMSE	R^2
				(W/m^2)	
Winter	-6.638	0.010	0.009	3.94	0.94
Spring	-0.160	0.007	0.007	2.84	0.95
Summer	2.554	0.000	0.007	2.89	0.94
Autumn	0.618	0.006	0.007	2.70	0.95

Conclusions

The US national anthropogenic heating database (available at https://geoplan.asu.edu/research-and-outreach/projects/AHdata) represents an important tool for urban climate modelers. One of the most significant limitations is the lack of spatial differentiation of the profiles within each city. Thus, we caution against the direct inclusion of the Q_f profiles developed in this manuscript into urban canopy models utilizing a multi-class urban representation. Users are urged to scale the city-specific data provided here appropriately, accounting for each urban land use class utilizing readily available classification data (in the US such detailed classifications are available from the National Land Cover Database; Fry *et al*., 2011).

Acknowledgements

MG was supported by National Science Foundation Grants EAR-1204774 and DMS-1419593, and U.S. Department of Agriculture NIFA grant 2015-67003-23508. The original methodological development (DJS and MAH) was supported by National Science Foundation Grant BCS-0410103.

References

Arguez, A., I. Durre, S. Applequist, R. S. Vose, M.F. Squires, X. Yin, R.R.J. Heim, T.W. Owen, (2012) NOAA's 1981-2010 U.S. Climate Normals, *Bulletin of the American Meteorological Society* 92 (11): 1687-1697.

Energy Information Administration (2010a) Electric Power Monthly, in: Energy Information Administration, U.S. Department of Energy, Washington DC.

Energy Information Administration (2010b) Natural Gas Monthly, in: Energy Information Administration, U.S. Department of Energy, Washington DC.

Flanner, M.G. (2009) Integrating anthropogenic heat flux with global climate models, *Geophysical Research Letters* 36 (2): L02801.

Fry, J. et al. (2011) Completion of the 2006 national land cover database for the conterminous United States, *Photogrammetric Engineering and Remote Sensing* 77(9): 858–864.

Hallenbeck, M., M. Rice, B. Smith, C. Cornell-Martinez, J. Wilkinson (1997) Vehicle Volume Distribution by Classification, in: Washington State Transportation Center (http://depts.washington.edu/trac), University of Washington, 1107 NE 45th St. Suite 535, Seattle WA 98105, Seattle, 1997, pp. 54.

Ichinose, T., K. Shimodozono, and K. Hanaki (1999) Impact of anthropogenic heat on urban climate in Tokyo, *Atmospheric Environment* 33: 3897-3909.

Klysik, K. (1996) Spatial and seasonal distribution of anthropogenic heat emissions in Lodz, Poland, *Atmospheric Environment* 30 (20) 3397-3404

Sailor, D.J., and L. Lu (2004) A top-down methodology for developing diurnal and seasonal anthropogenic heating profiles for urban areas, *Atmospheric Environment* 38 (17): 2737-2748.

Sailor, D. J., & Vasireddy, C. (2006) Correcting aggregate energy consumption data to account for variability in local weather. *Environmental Modelling & Software* 21(5): 733-738.

Sailor, D.J., M. Georgescu, J. Milne, and M. Hart, (2015) Development of a national anthropogenic heating database with an extrapolation for international cities, *Atmospheric Environment* 118: 7-18.

United States Department of Transportation (USDoT), Urbanized Areas – 2010: Miles and Daily Vehicle-Miles of Travel, in: Federal Highway Administration, U.S. Department of Transportation, 2013.

Effects of Urban Form and Atmospheric Stability on Local Microclimate

Introduction

The perspective of climate change increases the necessity of tackling the urban heat island (UHI) effects, by developing strategies to mitigate/adapt to changes. Although proper urban planning options could help minimize the effects of UHI, studies to adapt the built environment to these changes in urban areas are rare, particularly in the context of cool climate cities where urban warming is typically not seen as a current problem. This will change as the background climate continues to warm.

Analysing the influence of urban form on UHI could be a helpful way of reducing its negative consequences. While the exploration of the influence of urban form on local microclimate is helpful, it is necessary to untangle this effect from background atmospheric conditions that lead to such effects.

The present paper evaluates the effect of urban morphology (as measured by the Sky View Factor – SVF) on local climate according to atmospheric conditions exemplified by atmospheric stability – modified Pasquill-Gifford-Turner [PGT] classification system (Turner, 1970, modified by Mohan and Siddiqui, 1998) – in a cold climate city.

The increasingly urbanised nature of human habitation is contributing to worsening local climates. The intensity of climate change risks adds to this. Appropriate urban planning options could help ameliorate the heating problem and help "climate proof cities" for future climate change-related risks (Kleerekoper *et al*., 2012). In the context of cool climate cities, heat management (Stone *et al*., 2012) – both in terms of using the heat as a resource in winter and in terms of ameliorating its negative consequences in the summer – will be needed, in addition to climate change mitigation via greenhouse gas emission reduction. Nevertheless, the role of cities in climate change adaptation is only beginning to be addressed (for example: Hebbert and Jankovic, 2013) with city-specific urban climate change action plans remaining sketchy. In particular, urban form related studies to adapt to climate changes are rare (Shimoda, 2003).

In order to advance the importance of urban form manipulation to reduce the overheating risk it is necessary to explore the effectiveness of certain urban forms for this task and to clearly untangle the urban effect from the effect caused by atmospheric conditions. Krüger and Emmanuel (2013) estimated the effects of background atmospheric conditions on UHIs and intra-urban air temperature. They found that the range in intra-urban air temperature and relative warming at specific urban locations were accentuated after accounting for atmospheric stability. The relationship between the SVF and local warming was more pronounced under stable atmospheric conditions.

Table 1. Atmospheric stability classes PGT (adapted from Mohan and Siddiqui, 1998).

WS (m/s)	Daytime SR (W/m^2)				Night time CC (octas)		
	High[1]	Mod[2]	Low[3]	Cloudy	Low[4]	Mod[5]	High[6]
≤2	A	A-B	B	C	G-F	F	D
2-3	A-B	B	C	C	F	E	D
3-5	B	B-C	C	C	E	D	D
5-6	C	C-D	D	D	D	D	D
>6	C	D	D	D	D	D	D

WS: wind speed, SR global solar radiation, CC cloud cover, [1](>600), [2](300-600), [3](<300), [4](0-3), [5](4-7), [6](8), A (highly unstable or convective), B (moderately unstable), C (slightly unstable), D (neutral), E (moderately stable), and F (extremely stable), G (extremely stable, low wind).

Given the increasing interest in climate change adaptation as well as the increasing use of models to evaluate the efficacy of various adaptation actions (cf. Tomlinson *et al*., 2012) such assessment should account for both the urban as well as background atmospheric effects on microclimates.

The present paper presents the effect of atmospheric conditions as exemplified by atmospheric stability (modified Pasquill-Gifford-Turner classification system) and urban morphology as measured by the Sky View Factor (SVF) on intra-urban variations in air temperature in a cold climate city, in and around the mature urban area of Glasgow, UK (55° N, 4° W). The aim is to highlight their relative importance and to make preliminary explorations of the local warming effect of urban morphology under specific atmospheric stability classes.

Forty-nine locations were selected in the city centre, on the basis of SVF to represent a wide variety of urban forms (narrow streets, neighbourhood green spaces, urban parks, typical street canyons and public squares) and seven of these were assigned as locations for fixed weather stations. Thirty-one temperature measurement campaigns were made, using a 'traverse' method on a 'Meteobike' and on foot. The locations were chosen to represent a variety of urban formations (narrow streets, neighborhood greenspaces, urban parks, uniform and non-uniform street canyons and public squares). The visualization of local temperature variations was accomplished using Arc-Map tool from Arc-GIS package.

The present work indicates that the maximum intra-

urban temperature differences (i.e. temperature difference between the coolest and the warmest spots in a given urban region) are strongly correlated with atmospheric stability. It appears that atmospheric stability has a larger effect on intra-urban temperature variations than urban morphology in a cold climate city. The combined effect of the two provides interesting variations in local temperatures that may have urban planning implications, especially as the background climate continues to warm.

Methods and materials

The present study involved three tasks: the classification of atmospheric stability, determination of urban morphology and local temperature variations. Local temperature was measured at fixed locations as well as using a mobile traverse.

Atmospheric stability

The Pasquill-Gifford-Turner (PGT) (Table 1) classification system (Turner, 1970, modified by Mohan and Siddiqui, 1998) was adopted and the data was obtained from a weather station (Davis Vantage Pro2) in the Glasgow city centre (55° 51′ N, 4° 15′ W, 138m amsl – see Table 2 for details) to classify atmospheric stability.

Urban morphology

The determination of urban morphology was based on the Sky View Factor (SVF) computed by RayMan Pro (Matzarakis *et al*. 2007, Matzarakis *et al*. 2010). The images were taken by using fisheye-lens photographs (SIGMA 4.5mm f 2.8 EX). 49 locations representing a wide variety of urban formations (narrow streets, neighbourhood greenspaces, urban parks, uniform and non-uniform street canyons and public squares) were selected on the basis of SVF and seven of these were assigned as locations for fixed weather stations (see Table 3 for details). Figure 1 shows the location of all selected measurement points and the routes in three directions (east, central, west) which were defined to access all 42 points as quickly as possible.

Mobile temperature measurement protocol

Thirty-one temperature measurement campaigns were made during Spring and Summer 2013. In order to cover a large area of city centre within a relatively short time we used the 'traverse' method on three pre-determined routes (Figure 1), using a Tandem Recumbent Zöhrer model (termed here as a 'Meteobike,' Figure 2) and on foot.

All three routes started at Point 25 and ended at Point 10 (Figure 1) and spent two minutes at each measurement point. The first four measurements at each point were discarded to allow the data logger to stabilise. At a measurement interval of 10 seconds this gave eight

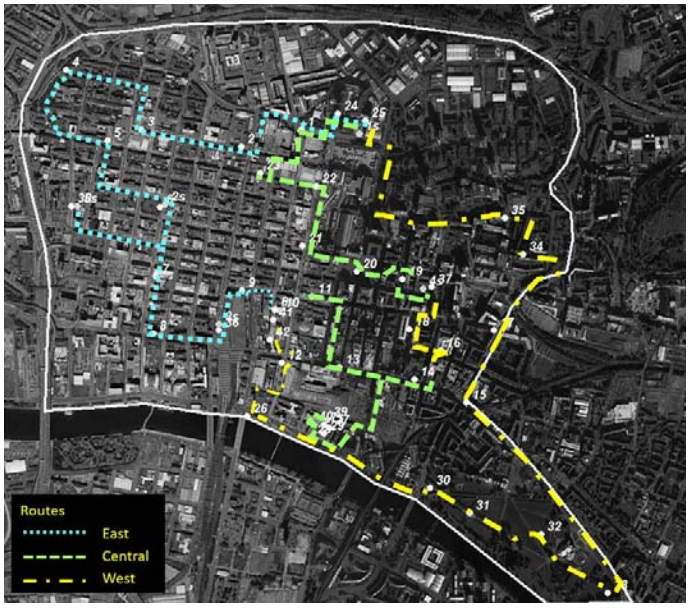

Figure 1. Measurement locations in Glasgow City Centre.

Figure 2. Meteobike.

measurements for each point which were then averaged. Measurement campaigns began at 2:30 p.m. local time (to be closer to the daily maximum temperature which typically occurred at 3:00 p.m. local time) and lasted approximately an hour. The logger characteristics of the weather station (WS) and data loggers (Tinytag TGP-4500) are shown in Table 4. They were housed in radiation shields (ACS-5050 - Stevenson Type Screen) to prevent direct and diffuse solar radiation falling on them.

Spatial representation of temperature variations

Measurement points were geo-referenced using a handheld GPS (GPS Garmin MAP). These were then transferred to a GIS map (ArcGIS v. 10.1) which itself was a combination of 2D (Lidar map, Edinburgh University, 2013) and 3D (Vector map, Landmap Spatial Discovery, 2013). Figure 3(a) and (b) shows these maps respectively.

The visualization of local temperature variations was accomplished using Arc-Map tool from Arc-GIS package. Figure 4 shows the temperature values for July 19th, 2013 and the sky view factor (SVF) for each measurement spot.

Table 2. Glasgow Caledonian University Weather Station (1s).

Coordinates and SVF	Fish-eye photo	Black and white mask	Solar path
Latitude: 55° 51′ 57″ N Longitude: 4° 15′ 0″ W **SVF: 0.774**			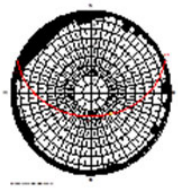

Table 3. Location of the stationary points (2s -7s).

Coordinates and SVF	Fish-eye photo	Black and white mask	Solar path
Blythswood Square (**POINT 2s**) Latitude: 55° 51′ 49″ N Longitude: 4° 15′ 44″ W **SVF: 0.017**	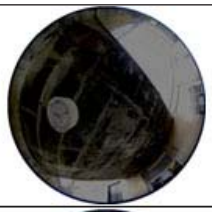	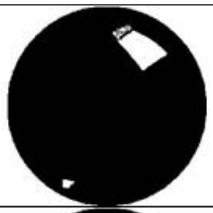	
City Council – Hope St (**POINT 3s**) Latitude: 55° 51′ 32″ N Longitude: 4° 15′ 33″ W **SVF: 0.201**			
City Council – Montrose St (**POINT 4s**) Latitude: 55° 51′ 38″ N Longitude: 4° 14′ 46″ W **SVF: 0.127**		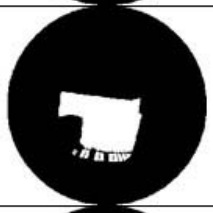	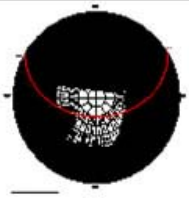
City Council – Elmbank St (**POINT 5s**) Latitude: 55° 51′ 49″ N Longitude: 4° 16′ 4″ W **SVF: 0.205**			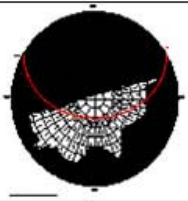
Lighthouse – Mitchell Ln (**POINT 6s**) Latitude: 55° 51′ 35″ N Longitude: 4° 15′ 20″ W **SVF: 0.042**			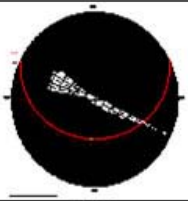
St Andrew's Cathedral (**POINT 7s**) Latitude: 55° 51′ 21″ N Longitude: 4° 15′ 9″ W **SVF: 0.440**			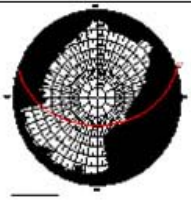

Table 4. Characteristics of the weather station (WS) and data loggers (Tinytag TGP-4500).				
Sensor	**Position**	**Resolution**	**Range**	**Accuracy**
Air temperature (WS)	Reference weather station	0.1°C to 1°C (selectable)	-40° to +65°C	±0.5°C
Air humidity (WS)	Reference weather station	1%	1 to 100%	±3-4%
Wind velocity (WS)	Reference weather station	0.4 m/s	1 to 80 m/s	±1 m/s
Wind direction (WS)	Reference weather station	22.5°	0 to 360°	±3°
Solar radiation (WS)	Reference weather station	1 W/m^2	0 to 1800 W/m2	±5°
Air temperature (Tinytag TGP-4500)	Traverses by bike or by foot and fixed points	0.01°C	-25°C at 85°C	±0.45°C

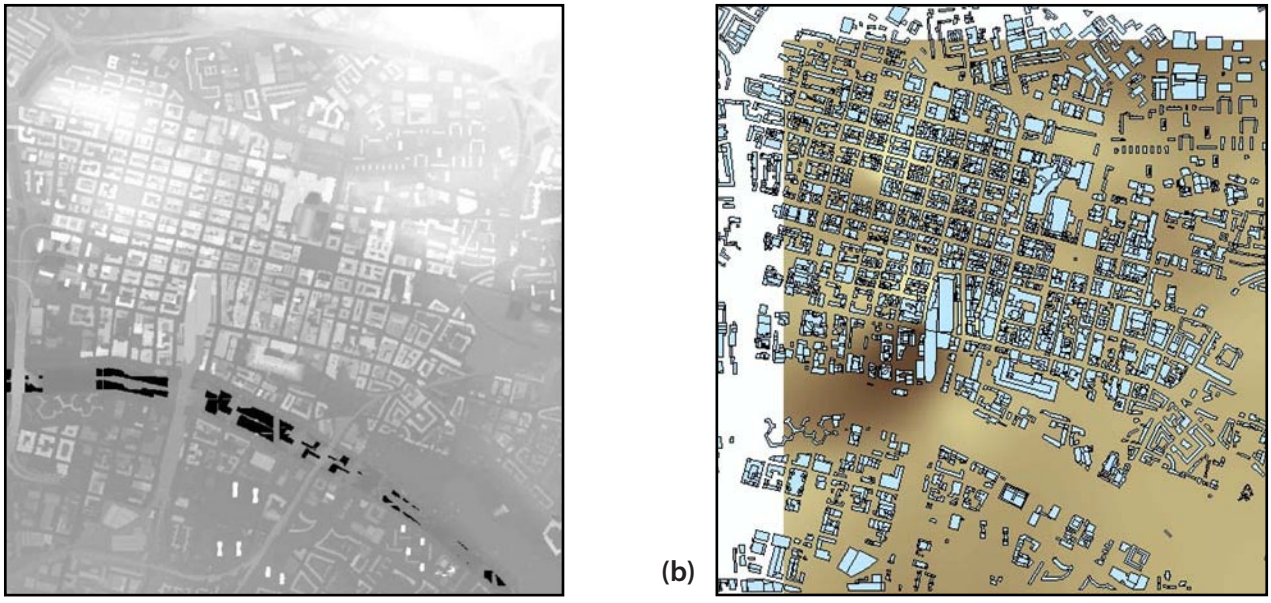

Figure 3. (a) Lidar map of Glasgow city centre, and (b) Vector map (blocks) with soil map.

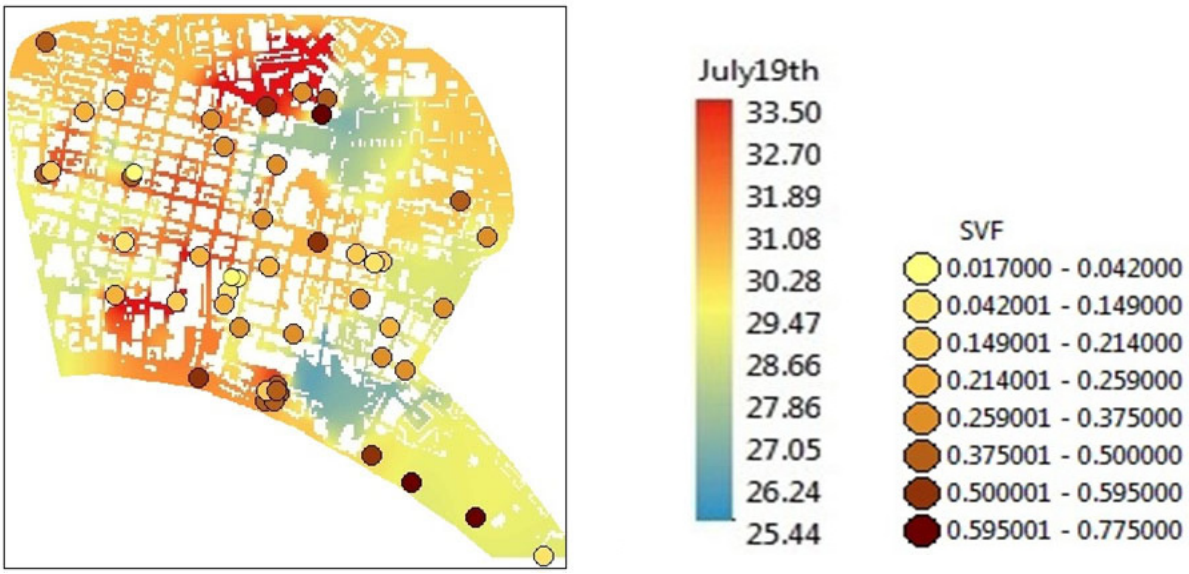

Figure 4. Air temperature variations on July 19th, 2013 and the SVF.

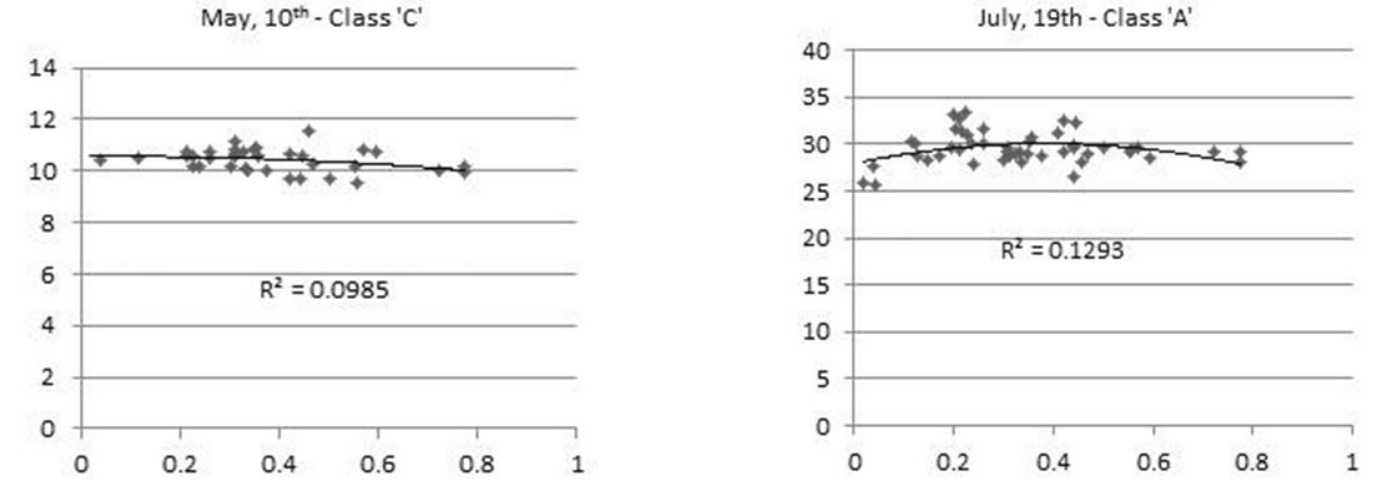

Figure 5. Temperature-SVF relationship on (a) coldest [Class C] and (b) hottest [Class A] days.

Results

In order to investigate the influence of atmospheric stability on local temperature, each measurement campaign was classified into relevant PGT Class (see Table 1 for the classification system). First results appeared inconclusive. Classes A-B and B exhibit the expected parabolic relationship (i.e. lower temperatures at very open – i.e. green and highly built-up i.e. shaded sites) during the day. However, this appears not the case with atmospheric stability classes A and C. The situation is similar when the variations on a very hot day (July 19th; maximum temperature difference with respect to the reference station = 7.70°C) and a cold day (May 10th; maximum temperature difference = 2.02°C) (see Figure 5).

However, the maximum temperature difference between the traverse points varied widely across the measurement campaigns (see Table 5). These differences (termed here as intra-urban temperature differences) varied between 1.96-7.70°C.

Figure 6 shows the relationship between maximum intra-urban temperature differences (°C) and atmospheric stability.

Here it is possible to observe that the presence of a highly unstable class ('A') is associated with the largest intra-urban temperature differences in Glasgow city centre. The more unstable the atmosphere the larger the intra-urban temperature variation. A high correlation between atmospheric class and air temperature difference can be noticed – $R^2 = 0.98$.

Table 6 presents average intra-urban temperature differences by atmospheric stability classes in scatter plots.

It may be seen that the relationships between SVF and intra-urban temperature differences are similar across all atmospheric stability classes (Range of R^2 = 0.4031-0.4308).

Discussion and conclusions

The present work indicates that the maximum intra-urban temperature differences (i.e. temperature difference between the coolest and the warmest spots in a given urban region) is strongly correlated with atmospheric stability. It appears that atmospheric stability has a larger effect on intra-urban temperature variations than urban morphology in a cold climate city. The combined effect of the two provides interesting variations in local temperatures that may have urban planning implications, especially as the background climate continues to warm.

The relationship between urban morphology (as measured by the SVF) and urban temperature variations, while being one of the most well studied aspect of UHI research, is not so clear. Atmospheric stability as defined by the PGT system, has an effect on the relationship between SVF and temperature but this relationship too needs additional clarification. SVF appears to have a 'parabolic' relationship with air temperature during daytime (both very open – green sites as well as heavily built up – shaded sites show lower temperatures), but this relationship is not conclusive. The more unstable atmospheric stability classes have the largest variations in urban temperatures while the less unstable classes exhibit smaller variations. All of the classes explain about half of the variations in urban temperatures. The spatial patterns in local temperature variations consistently show that water bodies and urban parks have consistently lower temperature variations. Thus, greenery and urban materials could play an important role in influencing the local climate in cold cities.

Knowing this limitation of urban morphology's influence on local temperature variations could be useful in devising realistic planning/design strategies to ameliorate urban overheating in the coming years as the background climate continues to warm.

Table 5. Maximum intra-urban temperature differences on measurement days.

Day	Class	Temperature difference	Day	Class	Temperature difference
May, 8th	C	2.35	June 18th	A-B	5.56
May 9th	C	2.29	June 19th	B	7.38
May 10th	C	2.02	June 25th	B	3.47
May 20th	B	4.84	June 26th	A-B	6.45
May 21th	A	7.20	June 27th	B	3.76
May 22th	A-B	4.99	July 1st	B	4.35
May 28th	C	1.96	July 3rd	C	3.28
May 29th	B	2.56	July 9th	C	3.28
May 30th	A-B	5.33	July 10th	A-B	3.25
June 5th	A-B	4.80	July 11th	A-B	2.89
June 6th	A-B	5.17	July 18th	A	7.05
June 7th	A-B	7.61	July 19th	A	7.70
June 10th	B	4.36	July 22th	A-B	4.71
June 11th	B-C	5.96	August13th	A-B	6.64
June 12th	B	4.26	August14th	C	3.68
June 17th	A-B	4.19			

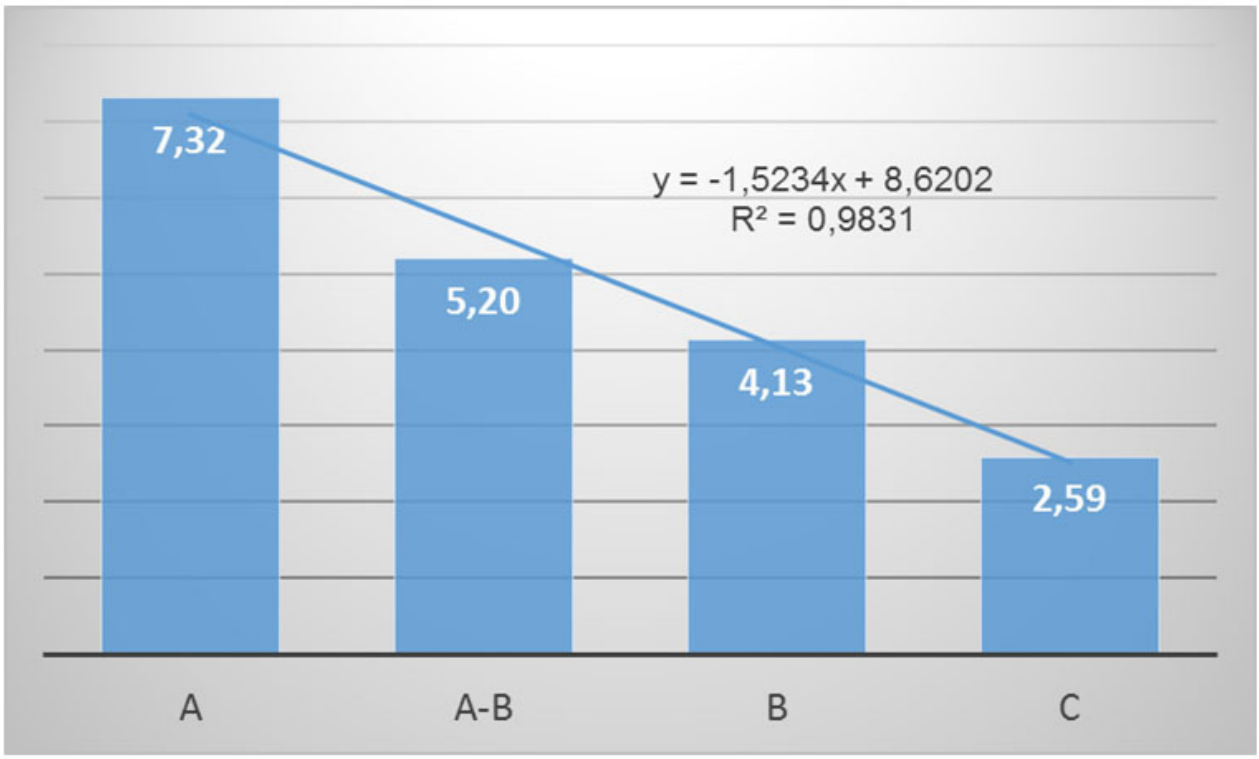

Figure 6. Maximum intra-urban temperatures vs. atmospheric stability.

Table 6. Distribution of temperature differences according to atmospheric stability classes.

Atmospheric Stability Class (PGT)	A	A-B	B	C
Average temperature difference (°C) vs. Sky View Factor	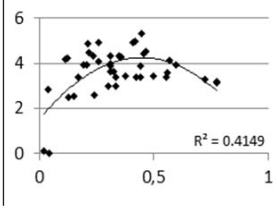	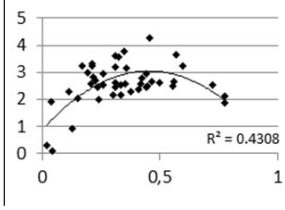	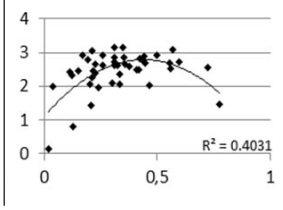	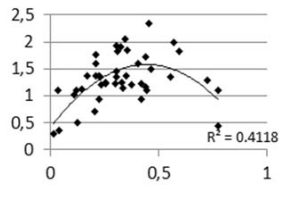

Acknowledgment

We gratefully acknowledge the financial help provided by the Brazilian funding agency CNPq (National Council for Scientific and Technological Development, Brazil Science without Borders 246551/2012-7) and facilities, instrumentation and analysis provided by the School of Engineering and Built Environment at Glasgow Caledonian University.

References

Edinburgh University, School of Informatics. URL: http://data.inf.ed.ac.uk/geo/lidar/ (accessed 06.15.13).

Hebbert M., Jankovic V. 2013. Cities and climate change: the precedents and why they matter. Urban Studies, 50, 1332-1347.

Kleerekoper L., van Esch M., Salcedo T. B. 2012. How to make a city climate-proof, addressing the urban heat island effect. Resources, Conservation and Recycling, 64, 30–38.

Krüger E., Emmanuel R. 2013. Accounting for atmospheric stability conditions in Urban Heat Island studies: the case of Glasgow, UK. Landscape and Urban Planning, 117, 112-121.

Matzarakis A, Rutz F, Mayer H. 2007. Modelling radiation fluxes in simple and complex environments - Application of the RayMan model. International Journal of Biometeorology, 51, 323–34.

Matzarakis A, Rutz F, Mayer H. 2010. Modelling radiation fluxes in simple and complex environments: basics of the RayMan model. International Journal of Biometeorology, 54(2), 131–139.

Mohan M., Siddiqui T. A. 1998. Analysis of various schemes for the estimation of atmospheric stability classification. Atmospheric Environment, 32(21), 3775-3781.

Shimoda Y. 2003. Adaptation measures for climate change and the urban heat island in Japan's built environment. Building Research and Information, 31, 222-230.

Tomlinson C. J., Chapman L., Thornes J. E., Baker C. J. 2012. Derivation of Birmingham's summer surface urban heat island from MODIS satellite images. International Journal of Climatology, 32, 214–224.

Turner D. B. 1970. Workbook of atmospheric dispersion estimates. Office of Air Program Pub. No. AP-26, Environmental Protection Agency, USA.

Patricia Drach
patricia.drach@gmail.com

PROURB/FAU, Federal University of Rio de Janeiro
Cidade Universitária, Brazil

Rohinton Emmanuel

School of Engineering & Built Environment,
Glasgow Caledonian University, Glasgow, UK

Climatic "memory" in the city of Jerusalem

Learning from the ancient olive trees of the historic Gethsemane garden

The Mount of Olives in Jerusalem rises to a height of more than 800 m above sea level – separating the Kidron Valley and walled Old City in the west from the Judean Desert and descent to the Dead Sea in the east. Its name, used from antiquity until today, comes from the olive trees that have grown on its slopes for thousands of years.

At the base of the Mount, the Gethsemane garden preserves a collection of olive trees of ancient origin – with the above-ground parts of eight of these trees having been dated to the twelfth century. Surprising evidence from genetic fingerprint analysis has shown that they share the same DNA, meaning that they were most likely propagated from the same genotype. Currently the olive trees appear to be healthy, but better knowledge of their immediate surroundings in terms of microclimate and air quality is important for understanding the environmental conditions that these trees have had to withstand, and to aid in the preservation of this natural heritage. For this purpose, the Institute for Biometeorology of the Italian National Research Council and the Italian Trees and Timber Institute are collaborating with *Custodia Terrae Sanctae* Franciscan Missionaries in Jerusalem to monitor the microclimate of the Gethsemane garden, and recently an agrometeorological weather station was installed in the proximity of the olive trees.

View of the Mount of Olives in Jerusalem, with the Gethsemane olive garden at the bottom left.

Ancient olive tree in Jerusalem's Gethsemane garden. The weather station is installed above the roof of the adjacent building, seen in the background.

Agrometeorological Weather Station

An automatic agrometeorological weather station (IBIMET-CNR, based on Campbell components) was installed on May 4th, 2016 on the roof of the convent building immediately adjacent to the Gethsemane olive tree garden. The position of the weather station was determined so as to ensure that high-quality weather data could be gathered as close as possible to the garden, and to provide the best possible accessibility given the technical and aesthetical limitations posed by such a location.

The weather station is equipped with sensors for the continuous measurement of air temperature (°C), relative humidity (%), rainfall (mm), wind speed (m/s), wind direction (deg), global solar radiation (W/m^2) and UVB solar radiation (W/m^2).

The climate of Jerusalem is classified as temperate with a dry summer season (Csa for Köppen and Geiger), with most rainfall in autumn and winter. From the data recorded during May-June 2016 we observe a characteristic *hamsin* induced by hot dry desert winds, with maximum temperatures of more than 40°C and very low humidity. These conditions generate high nightly temperatures as well, with minima over 20°C, due partly to heat retention by dense urban materials. Over the following days we observe extended heat wave conditions, with temperatures surpassing 35°C on multiple occasions.

Regarding precipitation, the dry season generally starts in April with only 24.5 mm average monthly rainfall, though the driest months are June, July and August (Israel Meteorological Service). From data recorded by

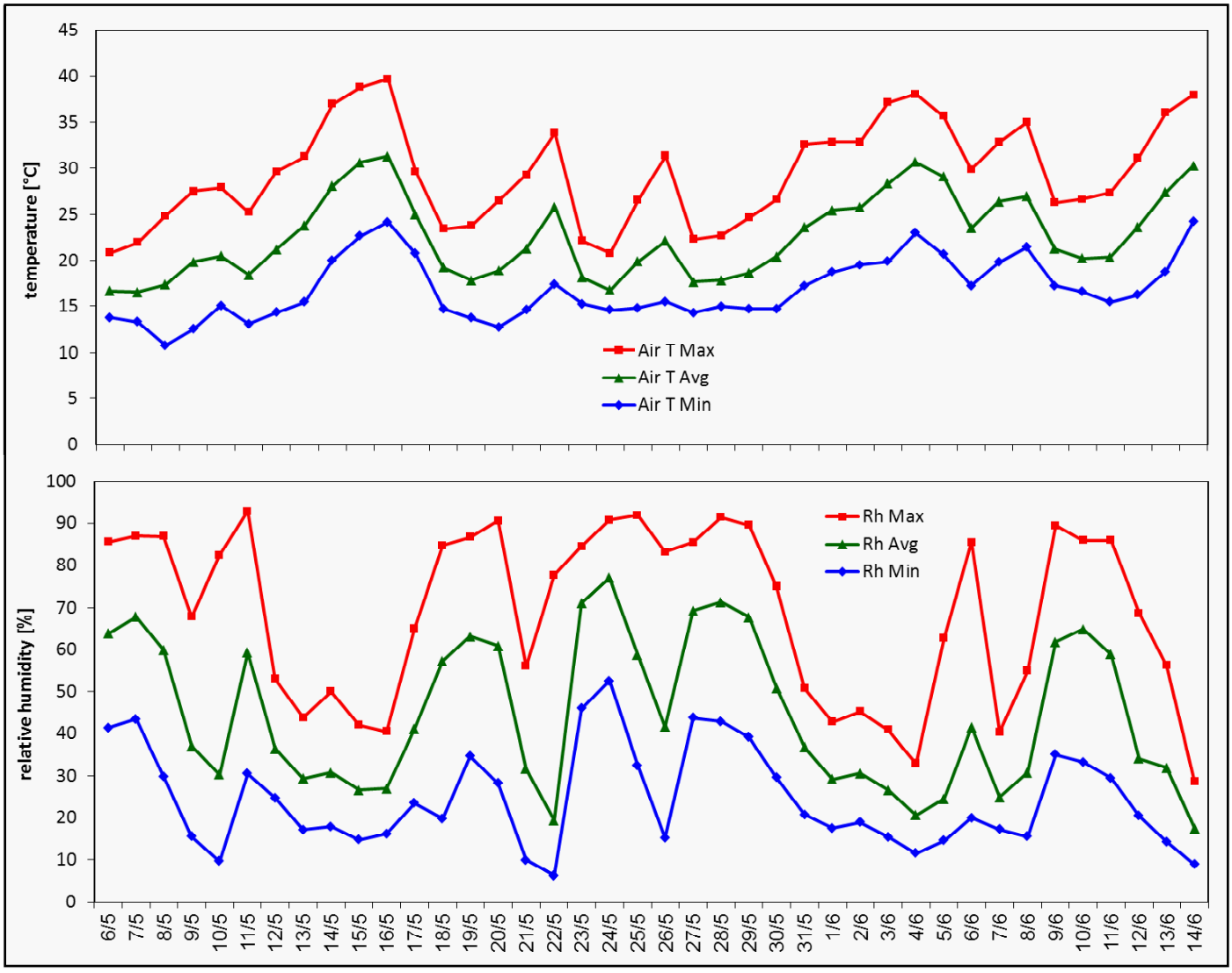

Daily ranges of air temperature and relative humidity measured by the weather station from May 6 to June 14, 2016.

the weather station, we can affirm that in the current year May was typically dry, with only 0.2 mm detected after the break of a heat wave on the night of May 24th, when the temperature had dropped rapidly and relative humidity was over 90%. At the same time, daily global solar radiation decreased abruptly and air temperature dropped by about 12°C compared to two days before.

To the east, the convent faces the mount's slope and a dense stand of cypress trees, which grow approximately to the height of the roof. These conditions possibly influence the overall air circulation, though the predominant wind direction is N-NW as a result of the regional morphology of the whole basin.

Studying the microclimate at Gethsemane will contribute to a better understanding of the trees' responses and resistance to such extreme weather conditions, and from an agronomical point of view to finding a relation between microclimate, phenology and productivity. For further information, contact Alessandro Zaldei (a.zaldei@ibimet.cnr.it).

Weather station installed on the roof of the Gethsemane convent, with the old city of Jerusalem in the background.

Recent Urban Climate Publications

Alizadeh-Choobari O, Ghafarian P, Adibi P (2016) Interannual variations and trends of the urban warming in Tehran. *Atmospheric Research* 170:176-185.

Alonzo M, McFadden JP, Nowak DJ, Roberts DA (2016) Mapping urban forest structure and function using hyperspectral imagery and lidar data. *Urban Forestry & Urban Greening* 17:135-147.

Bandala ER, Patino-Gomez C (2016) Appropriate technology and climate change adaptation. *Physics and Chemistry of the Earth*, Parts A/B/C 91:1.

Buchholz S, Kossmann M, Roos M (2016) INKAS – a guidance tool to assess the impact of adaptation measures against urban heat. *Meteorologische Zeitschrift* 25(3):281-289.

Chen Y-C, Chen C-Y, Matzarakis A, Liu J-K, Lin T-P (2016) Modeling of mean radiant temperature based on comparison of airborne remote sensing data with surface measured data. *Atmospheric Research* 174-175:151-159.

Daniels EE, Lenderink G, Hutjes RWA, Holtslag AAM (2016) Observed urban effects on precipitation along the Dutch West coast. *International Journal of Climatology* 36:2111-2119.

Gawuc L, Struzewska J (2016) Impact of MODIS Quality Control on Temporally Aggregated Urban Surface Temperature and Long-Term Surface Urban Heat Island Intensity. *Remote Sensing* 8(5):374.

Goodfriend E, Katopodes Chow F, Vanella M, Balaras E (2016) Large-Eddy Simulation of Flow Through an Array of Cubes with Local Grid Refinement. *Boundary-Layer Meteorology* 159:285-303.

Goulart EV, Coceal O, Branford S, Thomas TG, Belcher SE (2016) Spatial and Temporal Variability of the Concentration Field from Localized Releases in a Regular Building Array. *Boundary-Layer Meteorology* 159:241-257.

Haashemi S, Weng Q, Darvishi A, Alavipanah SK (2016) Seasonal Variations of the Surface Urban Heat Island in a Semi-Arid City. *Remote Sensing* 8:352.

Hu A, Levis S, Meehl GA, Han W, Washington WM, Oleson KW, van Ruijven BJ, He M, Strand WG (2016) Impact of solar panels on global climate. *Nature Climate Change* 6:290-294.

Jarden KM, Jefferson AJ, Grieser JM (2016) Assessing the effects of catchment-scale urban green infrastructure retrofits on hydrograph characteristics. *Hydrological Processes* 30:1536-1550.

Karsisto P, Fortelius C, Demuzere M, Grimmond CSB, Oleson KW, Kouznetsov R, Masson V, Järvi L (2016) Seasonal surface urban energy balance and wintertime stability simulated using three land-surface models in the high-latitude city Helsinki. *Quarterly Journal of the Royal Meteorological Society* 142:401-417.

In this edition a list is presented of publications that have generally come out between **March 2016 and May 2016**. As usual, papers published since this date are welcome for inclusion in the next newsletter and IAUC online database. Please send your references to the email address below with a header "IAUC publications" and the following format: Author, Title, Journal, Year, Volume, Issue, Pages, Dates, Keywords, URL, and Abstract. In order to make the lives of the Bibliography Committee members easier, please send the references **in a .bib format**.

Please note that we are still supporting (young) researchers to join and contribute to the Committee. If you are interested to join or would like to receive more information, please let me know via the email address below.

Regards,

Matthias Demuzere

Department of Earth and Environmental Sciences,
KU Leuven, Belgium

matthias.demuzere@ees.kuleuven.be

Keramitsoglou I, Kiranoudis CT, Sismanidis P, Zaksek K (2016) An Online System for Nowcasting Satellite Derived Temperatures for Urban Areas. *Remote Sensing* 8:306.

Kim DH, Rao PSC, Kim D, Park J (2016) 1/f noise analyses of urbanization effects on streamflow characteristics. *Hydrological Processes* 30:1651-1664.

Krehbiel C, Henebry GM (2016) A Comparison of Multiple Datasets for Monitoring Thermal Time in Urban Areas over the U.S. Upper Midwest. *Remote Sensing* 8:297.

Lee WK, Lee HA, Lim YH, Park H (2016) Added effect of heat wave on mortality in Seoul, Korea. *International Journal of Biometeorology* 60:719-726.

Li X, Li W, Middel A, Harlan SL, Brazel AJ, Turner II BL (2016) Remote sensing of the surface urban heat island and land architecture in Phoenix, Arizona: Combined effects of land composition and configuration and cadastral-demographic-economic factors. *Remote sensing of environment* 174:233-243.

Li X-B, Lu Q-C, Lu S-J, He H-D, Peng Z-R, Gao Y, Wang Z-Y (2016) The impacts of roadside vegetation barriers on the dispersion of gaseous traffic pollution in urban street canyons . Urban Forestry & Urban Greening 17:80 - 91.

Lu Y, Wang Q, Zhang Y, Sun P, Qian Y (2016) An estimate of anthropogenic heat emissions in China. *International*

Journal of Climatology 36:1134-1142.

Molenaar RE, Heusinkveld BG, Steeneveld GJ (2016) Projection of rural and urban human thermal comfort in The Netherlands for 2050. *International Journal of Climatology* 36:1708-1723.

Nosek S, Kukacka L, Kellnerová R, Jurcáková K, Janour Z (2016) Ventilation Processes in a Three-Dimensional Street Canyon. *Boundary-Layer Meteorology* 159:259-284.

Provencal S, Bergeron O, Leduc R, Barrette N (2016) Thermal comfort in Quebec City, Canada: sensitivity analysis of the UTCI and other popular thermal comfort indices in a mid-latitude continental city. *International Journal of Biometeorology* 60:591–603.

Psikuta A, Kuklane K, Bogdan A, Havenith G, Annaheim S, Rossi RM (2016) Opportunities and constraints of presently used thermal manikins for thermo-physiological simulation of the human body. *International Journal of Biometeorology* 60:435-446.

Qiu H, Tian L, Ho K-f, Yu ITS, Thach T-Q, Wong C-M (2016) Who is more vulnerable to death from extremely cold temperatures? A case-only approach in Hong Kong with a temperate climate. *International Journal of Biometeorology* 60:711-717.

Reyes B, Maxwell RM, Hogue TS (2016) Impact of lateral flow and spatial scaling on the simulation of semi-arid urban land surfaces in an integrated hydrologic and land surface model. *Hydrological Processes* 30:1192-1207.

Ryu Y-H, Bou-Zeid E, Wang Z-H, Smith JA (2016) Realistic Representation of Trees in an Urban Canopy Model. *Boundary-Layer Meteorology* 159:193-220.

Ryu Y-H, Smith JA, Bou-Zeid E, Baeck ML (2016) The Influence of Land Surface Heterogeneities on Heavy Convective Rainfall in the Baltimore-Washington Metropolitan Area. *Monthly Weather Review* 144:553-573.

Sachindra DA, Ng AWM, Muthukumaran S, Perera BJC (2016) Impact of climate change on urban heat island effect and extreme temperatures: a case-study. *Quarterly Journal of the Royal Meteorological Society* 142:172-186.

Shi L, Chu E, Anguelovski I, Aylett A, Debats J, Goh K, Schenk T, Seto KC, Dodman D, Roberts D, Roberts JT, VanDeveer SD (2016) Roadmap towards justice in urban climate adaptation research. *Nature Climate Change* 6:131-137.

Shi L, Liu P, Kloog I, Lee M, Kosheleva A, Schwartz J (2016) Estimating daily air temperature across the Southeastern United States using high-resolution satellite data: A statistical modeling study. *Environmental Researc*h 146:51-58.

Simiu E, Shi L, Yeo D (2016) Planetary Boundary-Layer Modelling and Tall Building Design. *Boundary-Layer Meteorology* 159:173–181.

Sismanidis P, Keramitsoglou I, Kiranoudis CT, Bechtel B (2016) Assessing the Capability of a Downscaled Urban Land Surface Temperature Time Series to Reproduce the Spatiotemporal Features of the Original Data. *Remote Sensing* 8:274.

Sisto NP, Ramirez AI, Aguilar-Barajas I, Magana-Rueda V (2016) Climate threats, water supply vulnerability and the risk of a water crisis in the Monterrey Metropolitan Area (Northeastern Mexico). *Physics and Chemistry of the Earth*, Parts A/B/C 91:2-9.

Song X-P, Sexton JO, Huang C, Channan S, Townshend JR (2016) Characterizing the magnitude, timing and duration of urban growth from time series of Landsat-based estimates of impervious cover. *Remote Sensing of Environment* 175:1-13.

Song Y, Liu H, Wang X, Zhang N, Sun J (2016) Numerical simulation of the impact of urban non-uniformity on precipitation. *Advances in Atmospheric Sciences* 33:783-793.

Theeuwes NE, Steeneveld G-J, Ronda RJ, Holtslag AAM (2016) A diagnostic equation for the daily maximum urban heat island effect for cities in northwestern Europe. *International Journal of Climatology* n/a–n/a.

Theeuwes NE, Steeneveld G-J, Ronda RJ, Rotach MW, Holtslag AAM (2015) Cool city mornings by urban heat. *Environmental Research Letters* 10:114022.

Tomas JM, Pourquie MJBM, Jonker HJJ (2016) Stable Stratification Effects on Flow and Pollutant Dispersion in Boundary Layers Entering a Generic Urban Environment. *Boundary-Layer Meteorology* 159:221–239.

Tominaga Y, Blocken B (2016) Wind tunnel analysis of flow and dispersion in cross-ventilated isolated buildings: Impact of opening positions. *Journal of Wind Engineering and Industrial Aerodynamics* 155:74-88.

Trusilova K, Schubert S, Wouters H, Früh B, Grossman-Clarke S, Demuzere M, Becker P (2016) The urban land use in the COSMO-CLM model: a comparison of three parameterizations for Berlin. *Meteorologische Zeitschrift* 25:231-244.

Wang C, Myint SW, Wang Z, Song J (2016) Spatio-Temporal Modeling of the Urban Heat Island in the Phoenix Metropolitan Area: Land Use Change Implications. Remote Sensing 8(3):185.

Welker C, Martius O, Stucki P, Bresch D, Dierer S, Brönnimann S (2016) Modelling economic losses of historic and present-day high-impact winter windstorms in Switzerland. *Tellus A* 68.

Wu J, Zha J, Zhao D (2016) Estimating the impact of the changes in land use and cover on the surface wind speed over the East China Plain during the period 1980-2011. *Climate Dynamics* 46:847-863.

Yi C, Kim KR, An SM, Choi Y-J, Holtmann A, Jänicke B, Fehrenbach U, Scherer D (2016) Estimating spatial patterns of air temperature at building-resolving spatial resolution in Seoul, Korea. *Int. Journal of Climatology* 36:533-549.

Zuvela-Aloise M, Koch R, Buchholz S, Fruh B (2016) Modelling the potential of green and blue infrastructure to reduce urban heat load in the city of Vienna. *Climatic Change* 135:425-438.


Spring 2016 in Florence, Italy

Upcoming Conferences...

FIRST INTERNATIONAL CONFERENCE ON URBAN PHYSICS (FICUP)
Quito - Galápagos • Sept 25 - Oct 2, 2016
http://www.ficup2016.com/

2ND URBAN & INFRASTRUCTURE DEVELOPMENT CONFERENCE FOR EAST AND CENTRAL AFRICA
Kampala, Uganda • October 5-6, 2016
http://uidc.siup.ac.ug/

JOINT URBAN REMOTE SENSING EVENT (JURSE 2017)
Dubai, UAE • March 5-7, 2017
http://jurse2017.com/

GREEN INFRASTRUCTURE: NATURE BASED SOLUTIONS FOR SUSTAINABLE & RESILIENT CITIES
Orvieto, Italy • April 4-7, 2017
http://www.greeninurbs.com/finalconference/

13TH SYMPOSIUM ON THE URBAN ENVIRONMENT AT THE AMS 97TH ANNUAL MEETING
Seattle, WA USA • January 22–26, 2017
https://annual.ametsoc.org/2017/index.cfm/programs/conferences-and-symposia/13th-symposium-on-the-urban-environment/

Call for Papers

The theme for the 2017 AMS Annual Meeting is "Observations Lead the Way". Under the auspices of the proposed theme, topics related to advances in observations, modeling, and applications can be explored at the 13th Symposium on the Urban Environment. Papers and posters are invited on all subjects dealing with urban environment issues, including in-situ and remote-sensing observations, modeling, theoretical, forecasting, and applied studies such as societal and economic impacts of urbanization.

Abstract Submissions: by August 1, 2016

IAUC and WMO sign a new agreement of cooperation

Recently, the IAUC and WMO signed a new agreement of cooperation. This new agreement builds on an earlier agreement that was initiated by IAUC President Matthias Roth during his term. The WMO has decided recently that urban activities should be an integral part of all the priorities of the WMO Strategic Plan for 2016-19, so as to strengthen cross-sectorial climate services in urban areas.

This new focus is in support of the United Nations New Urban Agenda. The intent is to give cities the tools they need to reduce emissions, build safe, healthy and resilient communities and implement UN Sustainable Development goals. To achieve this goal, the WMO is seeking to build services that can meet the special needs of cities through a combination of dense observation networks, high-resolution weather forecasts, multi-hazard early warning systems, and climate services.

The intent is to give cities the tools they need to reduce emissions, build safe, healthy and resilient communities and implement UN Sustainable Development goals.

The agreement, which lasts for an initial period of fiveyears, is intended to help facilitate the WMO mission of encouraging research and training in meteorology and the coordination of international aspects of such research and training, including related fields, such as urban meteorology. As a first action, IAUC has assisted WMO with a proposal for a Roundtable on "Building Climate Smart Cities" as part of the UN Habitat III Conference.

I welcome this new focus on the part of WMO and I think it fits well with the objectives of IAUC. I would like to acknowledge the significant effort that Alexander Baklanov at WMO, a member of our IAUC Board, has made in revitalizing this agreement and in the proposal to UN Habitat III. I hope IAUC members will join me in supporting this new cooperation and will contribute to future initiatives that may be proposed under this agreement.

– James Voogt, IAUC President

Newsletter Contributions

The next edition of ***Urban Climate News*** will appear in late September. Contributions for the upcoming issue are welcome, and should be submitted by August 31, 2016.

Editor: David Pearlmutter (davidp@bgu.ac.il)

News: Paul Alexander (paul.alexander@nuim.ie)

Conferences: Jamie Voogt (javoogt@uwo.ca)

Bibliography: Matthias Demuzere (matthias.demuzere@ees.kuleuven.be)

Projects: Sue Grimmond (Sue.Grimmond@kcl.ac.uk)

Submissions should be concise and accessible to a wide audience. The articles in this Newsletter are unrefereed, and their appearance does not constitute formal publication; they should not be used or cited otherwise.